

Disentangling the role of environmental processes in galaxy clusters

Jonathan D. Hernández-Fernández¹, J. M. Vílchez¹, and J. Iglesias-Páramo^{1,2}

Received _____; accepted _____

¹Instituto de Astrofísica de Andalucía, Glorieta de la Astronomía s/n, 18008 Granada;
jonatan@iaa.es

²Centro Astronómico Hispano Alemán C/ Jesús Durbán Remón, 2-2 04004 Almería

ABSTRACT

In this work we present the results of a novel approach devoted to disentangle the role of the environmental processes affecting galaxies in clusters.

This is based on the analysis of the $NUV - r'$ distributions of a large sample of star-forming galaxies in clusters spanning more than four absolute magnitudes. The galaxies inhabit three distinct environmental regions: virial regions, cluster infall regions and field environment.

We have applied rigorous statistical tests in order to analyze both, the complete $NUV - r'$ distributions and their averages for three different bins of r' -band galaxy luminosity down to $M_{r'} \sim -18$, throughout the three environmental regions considered.

We have identified the environmental processes that significantly affect the star-forming galaxies in a given luminosity bin by using criteria based on the characteristics of these processes: their typical time-scales, the regions where they operate and the galaxy luminosity range for which their effects are more intense.

We have found that the high-luminosity ($M_{r'} \leq -20$) star-forming galaxies do not show significant signs in their star formation activity neither of being affected by the environment in the last $\sim 10^8$ yr nor of a sudden quenching in the last 1.5 Gyr.

The intermediate-luminosity ($-20 < M_{r'} \leq -19$) star-forming galaxies appear to be affected by starvation in the virial regions and by the harassment both, in the virial and infall regions.

Low-luminosity ($-19 < M_{r'} \leq -18.2$) star-forming galaxies seem to be affected by the same environmental processes as intermediate-luminosity star-forming galaxies in a stronger way, as it would be expected for their lower luminosities.

Subject headings: galaxy - galaxy cluster - environment - multi-wavelength - SED

1. Introduction

The influence of the environment on galaxies involves a rich variety of processes that include the interactions of galaxies with other components of the Universe: other galaxies, the intra-cluster medium (ICM) or the cluster/group dark matter haloes (DMHs). As a result of the different studies devoted to shed light on this key issue of the Extragalactic Astronomy, a number of reviews have become available in the recent years (Treu et al. 2003; Poggianti 2006; Boselli & Gavazzi 2006; Mo et al. 2010). As a reference, Treu et al. (2003) split the environmental processes into three groups:

- Galaxy-ICM interactions dominate the gas stripping processes, where the interstellar medium of galaxies is stripped via various mechanisms, including viscous and turbulent stripping, thermal evaporation and ram-pressure stripping (Boselli & Gavazzi 2006). Galaxy-ICM interactions can also trigger star formation through the compression of galactic gas clouds (Dressler & Gunn 1983; Evrard 1991; Fujita 1998). The ICM stripping of the hot halo gas results in a subsequent quenching of star formation (Bekki et al. 2002).
- Galaxy-cluster gravitational interactions can tidally compress the galaxy envelope of gas and increase the star formation rate (Byrd & Valtonen 1990; Henriksen & Byrd 1996; Fujita 1998). The galaxy starvation can be enhanced by the tidal interaction with the cluster DMH which contributes to the removal of the hot gas halo of the galaxy (Bekki et al. 2002). The tidal truncation of the external galaxy regions due to the action of the cluster potential produces a late quenching of star formation along a few Gyr if the galaxy reservoir is removed. However, their effects are more clearly observed in the structural changes of the mass profile (Merritt 1984; Ghigna et al. 1998; Natarajan et al. 1998).

- Tidal galaxy-galaxy interactions dominate the galaxy mergers or strong galaxy encounters (Icke 1985; Mihos 1995; Bekki 1998) and the galaxy harassment (Moore et al. 1996, 1999, 1998).

These three groups of processes have associated different spatial/time scales and characteristics which we describe below:

- Time-scales. We can distinguish between long and short-time-scale processes. Following the scheme proposed by Poggianti (2006), the long time-scale processes embrace the gas stripping processes and the galaxy mergers or strong galaxy interactions and the long-time-scale processes embrace the galaxy starvation (Larson et al. 1980; Bekki et al. 2002) and the galaxy harassment (Moore et al. 1996). The time-scale for suppression of star formation in gas stripping goes from $\sim 10^7$ yr (Abadi et al. 1999) to 10^8 yr (Quilis et al. 2000) for a Milky Way-like galaxy. In galaxy mergers, both the encounter time and the duration of the starburst phase have a time-scale of the order of 10^7 yr (Mihos & Hernquist 1994, 1996). Numerical simulations (Bekki et al. 2002) indicate that the starvation combining the interaction with the ICM and the cluster potential has a time-scale of several Gyr. Galaxy harassment takes place along several cluster crossing times, i.e. a few gigayears (Boselli & Gavazzi 2006; Moore et al. 1998, Appendix A).
- Spatial-scales. Also we can distinguish between long and short spatial-scale processes. The galaxy starvation and the galaxy harassment have spatial-scales of the order of virial radius or longer (Treu et al. 2003; Boselli & Gavazzi 2006). In the gas stripping, the cold gas of galaxies interacts hydrodynamically with the ICM from its vicinity, though this occurs along the way crossing the ICM of the virial region, thus it is assumed to be a long spatial-scale process. The main small-scale environmental

processes are the galaxy mergers or galaxy-galaxy tidal interactions which occur in a spatial scale that is of the order of the size of galaxies.

- **Environments.** Certain environmental processes operate more efficiently or occur more frequently in certain types of environments or places. The starvation or the gas stripping operate preferably in the central regions of clusters, where the ICM drag force and the cluster tidal forces are enough to strip the gas components of the galaxy. The galaxy harassment rate f_h scales with the luminous galaxy density ρ_{gal} and mass M_* as $f_h \propto \rho_{gal} M_*^2 \propto \rho_{gal} r^2$. In the simple case where local density scales smoothly as r^{-2} , the harassment rate should be independent of the cluster radius (Treu et al. 2003). The merging processes are most efficient when the relative velocities between the galaxies are low, thus they are expected to be more efficient in galaxy groups than in the inner regions of clusters. The galaxy groups infalling to clusters represent ideal places for an environmental-driven galaxy evolution in the frame of a "preprocessing" scenario (Cortese et al. 2004; Mihos 2004).
- **Galaxy luminosity range.** In addition to this, it has to be taken into account that the effect of the different processes depend on the galaxy luminosities, some of them are more efficient operating on bright/giant galaxies (gas stripping, Quilis et al. 2000) and other processes affecting to dwarf and low-surface brightness galaxies (galaxy harassment, Moore et al. 1999).

These physical processes have been proposed/invoked in order to explain numerous observational facts pointing out that the environment in which a galaxy inhabits has a profound impact on its evolution in terms of defining both its structural properties and its star formation histories. Perhaps the two most remarkable observational results are the morphology-density relation - the fraction of early-type galaxies increases towards high-density environments - (Dressler 1980) and the star formation-density relation - the

fraction of star-forming galaxies as well as the intensity of the star formation per galaxy decreases towards high-density environments - (Lewis et al. 2002; Gómez et al. 2003; Rines et al. 2005).

The UV luminosity has revealed as a good proxy of the recent star formation because it comes from the more short-lived stars $\tau < 10^8$ yr (Kennicutt 1998; Kauffmann et al. 2007; Martin et al. 2005). Hence, we can trace time variations of around 100 Myr in the star formation history of a galaxy using the ultraviolet luminosity (Leitherer et al. 1999) and/or UV-optical colors (Kaviraj et al. 2007b,a). The UV luminosity is strongly linked to the FIR luminosity ($\sim 8\text{-}1000 \mu\text{m}$), the UV radiation emitted by the young stellar populations is strongly absorbed by dust in the star-forming molecular clouds and reemitted through IR photons. So, both the UV-to-FIR luminosity budget as a proxy of the attenuation suffered by the young stellar population (see Buat et al. 2005) or the bolometric luminosity from the young stellar populations $L_{BOL} = L_{UV} + L_{FIR}$ as a proxy of the star formation rate (Wang & Heckman 1996; Iglesias-Páramo et al. 2006) also give important insights on the star formation activity of galaxies.

On the other hand, assuming that field galaxies are the galaxies less affected by the influence of the environment, we can take a sample of field galaxies as a fiducial sample (approximated) free from interactions i.e. in absence of environmental influence. Therefore, if the distribution of a UV-optical color of a star-forming galaxy sample (i.e. those with blue UV-optical colors, e.g. Haines et al. 2008; Chilingarian & Zolotukhin 2012) is statistically different from the corresponding distribution for a field star-forming galaxy sample (at the same cosmic time), we can conclude those galaxies are suffering a significant change in their star formation level in a time-scale of around 10^8 yr or longer. Assuming this fact, we develop a original approach which permit us assign the intensity of those environmental processes affecting the galaxies depending on their luminosity by means of

the analysis of the variations of the distributions of a UV-optical color of star-forming galaxies throughout different environmental regions. We choose the UV-optical color $NUV - r'$ because these two spectral bands trace two different time-scales of the star formation history; the NUV-band traces a $\tau \sim 10^8$ yr and the r' -band a more long time-scale $\tau \sim 10^9 - 10^{10}$ yr (Kennicutt 1998; Martin et al. 2005). Because of this, $NUV - r'$ shows a tight correlation with the ratio of the recent star formation over the past-averaged star formation (Salim et al. 2005).

The remainder of the paper is organized as follows: in section 2, we describe the photometric data and the sample of galaxies in clusters used in this work. In section 3, we present the main results derived from the $NUV - r'$ distributions of our sample of galaxies. Section 4 presents the discussion of the implications resulting from our analysis. In section 5, we summarize the main results and conclusions of this work.

2. The sample of cluster galaxies

This work is based on data compiled from the SDSS-DR6 (Adelman-McCarthy et al. 2008) and GALEX-AIS (Martin et al. 2005) for a sample of cluster galaxies extensively described in Hernández-Fernández et al. (2012, hereafter Paper I). This sample consists on a total of ~ 5000 galaxies from 16 nearby clusters ($z < 0.05$) showing a rich variety in their characteristics, from poor to rich clusters with cluster velocity dispersions between $200 \lesssim \left(\frac{\sigma_c}{\text{km s}^{-1}}\right) \lesssim 800$. The basic properties of these clusters are listed in Table 1. The galaxies span a luminosity range containing the classical luminosity boundary between giant and dwarf galaxies $M_B \sim -18$. The selection of the clusters was constrained by the condition that they were covered by SDSS-DR6 and GALEX-AIS throughout sky areas corresponding to physical sizes of several virial radii, i.e. several Mpc. This condition ensures that our sample of galaxies probes different environments from the central regions of rich clusters

to the low-density field, including the galaxy structures around clusters as groups, sheets and filaments. The Main Galaxy Sample of SDSS (Strauss et al. 2002) consists of those galaxies with r' -band petrosian magnitudes $r' < 17.77$ and r' -band petrosian half-light surface brightnesses $\mu < 24.5$ mag arcsec⁻², retrieved from the imaging survey which has a 95% completeness limit for stars of $r' = 22.2$ (Stoughton et al. 2002). GALEX has performed the first space UV imaging all-sky survey in two bands (FUV:1350-1750 Å and NUV:1750-2750 Å) down to a Galactic-extincted magnitude of $m_{AB} = 20.5$. The broad-band photometry from both SDSS-DR6 and GALEX-AIS is carefully chosen to retrieve the total integrated flux for each galaxy in the selected band. For the SDSS photometry, we choose the composite-model magnitude, which is a weighted linear combination of the fluxes extracted with a *De Vaucouleurs* profile and an exponential radial profile fit to the surface brightness profile of each galaxy (Abazajian et al. 2004). For the GALEX photometry, we choose the elliptical aperture photometry (MAG_AUTO option in SExtractor code, Bertin & Arnouts 1996) in order to include the total integrated UV flux for each galaxy source.

3. Results: UV-optical color distribution of cluster galaxies

The main goal of this work is to characterize the role of the environment in the star formation properties of a sample of cluster galaxies with active star formation. As a first step we select the star forming galaxies from the total cluster galaxy sample previously described. For this we apply the UV-optical color cut proposed for the $(NUV - r')$ vs. $(u' - r')$ color-color diagram in Paper I. We assume a galaxy is a star-forming galaxy whether its colors fulfill the following prescription:

$$\text{STAR - FORMING : } \begin{cases} NUV - r' < 4.9 & , \text{ for } u' - r' < 2.175 \\ NUV - r' < -2(u' - r') + 9.25 & , \text{ for } u' - r' > 2.175 \end{cases}$$

Table 1: Main properties of the cluster sample.

ID_{NED}	$\alpha(J2000)$	$\delta(J2000)$	z_{med}	σ_c	r_{200}	n_{tot}	θ_{tot}	$\log(L_X)$
	deg	deg		km s ⁻¹	Mpc		deg	L _⊙
(1)	(2)	(3)	(4)	(5)	(6)	(7)	(8)	(9)
UGC1 141	138.499	30.2094	0.0228	501.8	1.21	413	4.159	42.12
WBL 245	149.120	20.5119	0.0255	86.7	0.20	88	3.720	...
UGC1 148 NED01	142.366	30.2139	0.0263	316.7	0.76	354	3.606	...
ABELL 2199	247.154	39.5244	0.0303	756.2	1.83	1104	3.125	44.85
WBL 213	139.283	20.0403	0.0290	537.1	1.29	548	3.266	≤41.9
WBL 514	218.504	3.78111	0.0291	633.7	1.52	580	3.257	43.18
WBL 210	139.025	17.7242	0.0287	433.3	1.06	402	3.298	43.22
WBL 234	145.602	4.27111	0.0291	243.6	0.58	87	3.262	...
WBL 205	137.387	20.4464	0.0288	679.8	1.60	527	3.289	...
UGC1 393	244.500	35.1000	0.0314	637.9	1.52	529	3.016	43.60
UGC1 391	243.352	37.1575	0.0330	407.0	0.97	637	2.874	...
B2 1621+38:[MLO2002]	245.583	37.9611	0.0311	607.3	1.46	1053	3.046	43.19
UGC1 271	188.546	47.8911	0.0305	323.2	0.72	181	3.104	...
ABELL 1185	167.699	28.6783	0.0328	789.3	1.90	754	2.894	43.58
ABELL 1213	169.121	29.2603	0.0469	565.7	1.35	305	2.021	43.77
UGC1 123 NED01	127.322	30.4828	0.0499	849.0	2.00	260	1.900	44.32

(1) NED identifier, (2) and (3) Celestial coordinates of cluster center from NED webpage, (4) Cluster average redshift, (5) Cluster velocity dispersion, (6) Radius 200, (7) No. of observed galaxies associated to each cluster, (8) Half size of sky square region retrieved for each cluster, computed assuming the Local Universe approximation $cz=HD$, the small-angle approximation $D_P=D\times\theta[\text{rad}]$ and a projected radius $R_P=7.1$ Mpc (9) Bolometric X-ray luminosity from Mahdavi & Geller (2001) except for WBL 213 (Mahdavi et al. 2000).

As can be seen in Figure 1, this boundary appears more appropriate to segregate star-forming galaxies from passive galaxies than the optical cut in the $u' - r'$ color proposed by Strateva et al. (2001).

The next step is to define three regions where different physical processes are expected to act in a different way and intensity due to the different environmental conditions: the cluster virial regions, the cluster infall regions and the field environment. In order to select galaxies from each environment, we take advantage from their spatial \tilde{r} and velocity \tilde{s} variables through the phase diagram:

$$(\tilde{s}, \tilde{r}) \equiv \left(\left(\frac{c(z - z_{med})}{\sigma_c} \right), \left(\frac{R_P}{r_{200}} \right) \right) \quad (1)$$

being c the light speed, the z galaxy redshift, z_{med} cluster redshift, σ_c cluster velocity dispersion, R_P physical projected radius from cluster center and r_{200} the virial radius.

In this phase diagram, galaxies in clusters are located inside the region delimited by a bi-valued caustic $\tilde{s} = \pm \mathcal{A}(\tilde{r})$ with a characteristic trumpet shape symmetrical with respect to the \tilde{r} -axis (Kaiser 1987); outside the caustic limits, the density of galaxies drops substantially. Galaxies outside the caustics are background or foreground galaxies (e.g. den Hartog & Katgert 1996). Rines et al. (2003) numerically compute the caustic $\mathcal{A}(\tilde{r})$ for a sample of galaxy clusters in the Local Universe (see their figure 4), using the method proposed by Diaferio (1999). This caustic curve can be accurately approximated by the following terms:

$$\mathcal{A}(\tilde{r}) = \begin{cases} 2.5 - \frac{5}{7}\tilde{r} & , \text{ for } \tilde{r} \leq 2.30 \\ 1.0 - \frac{1}{16}\tilde{r} & , \text{ for } \tilde{r} > 2.30 \end{cases}$$

Following Rines et al. (2003), we define the three different environments studied here in the following way:

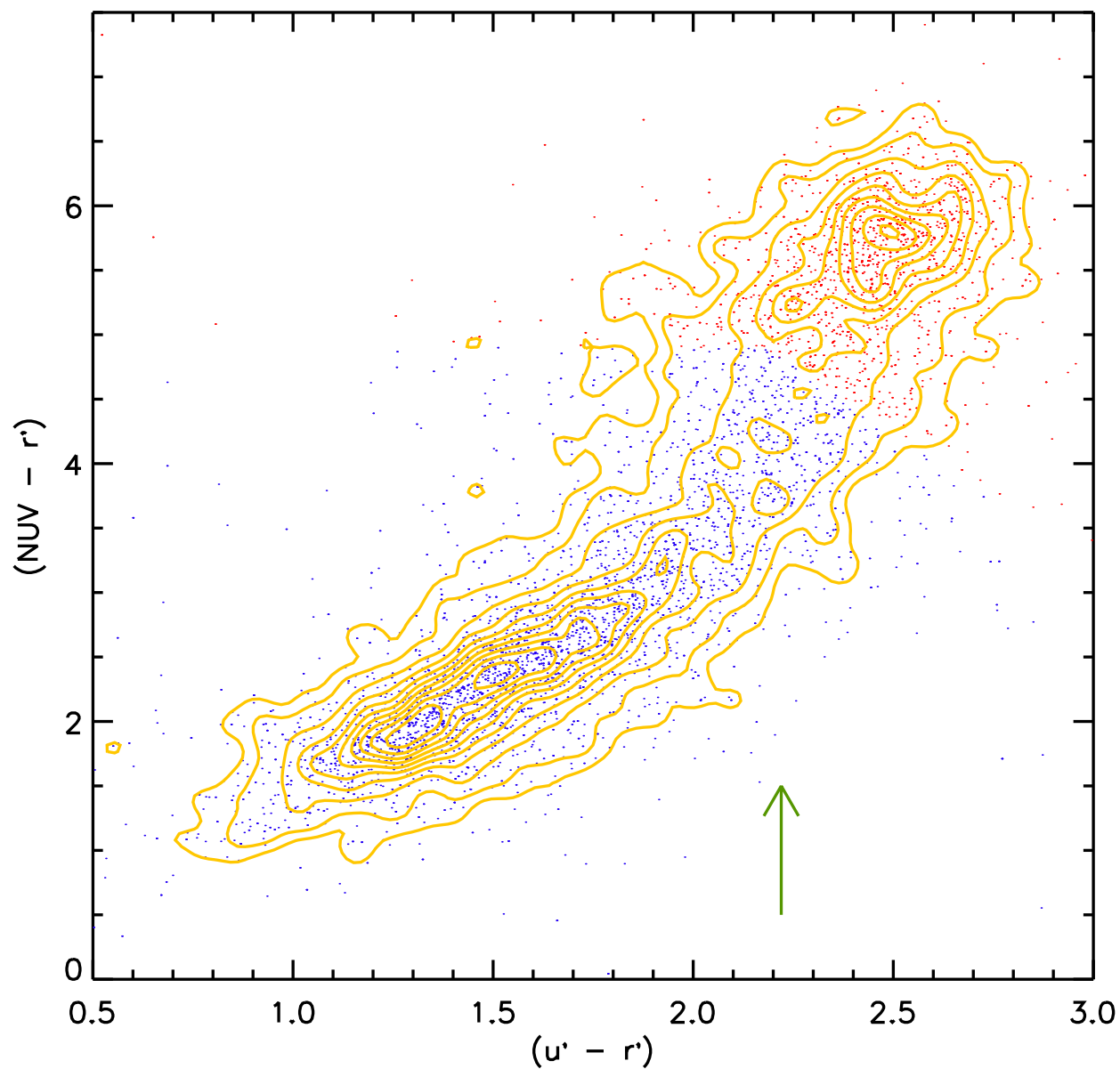


Fig. 1.— $(NUV - r')$ vs. $(u' - r')$ for the sample of galaxies. Yellow isocontours represents the isodensity contours of galaxies. Green dashed broken line is the UV-optical color-color cut proposed in Paper I. Green vertical arrow points out to the $u' - r'$ cut proposed by Strateva et al. (2001). Blue and red points represent, respectively, star-forming and passive galaxies under the prescription shown in Section 3.

$$\begin{aligned}
 \text{Virial regions:} & \quad -\mathcal{A}(\tilde{r}) \leq \tilde{s} \leq +\mathcal{A}(\tilde{r}) \quad \wedge \quad \tilde{r} \leq 1 \\
 \text{Infall regions:} & \quad -\mathcal{A}(\tilde{r}) \leq \tilde{s} \leq +\mathcal{A}(\tilde{r}) \quad \wedge \quad 1 < \tilde{r} \leq 5 \\
 \text{Field environment:} & \quad \tilde{s} < -\mathcal{A}(\tilde{r}) \quad \wedge \quad +\mathcal{A}(\tilde{r}) < \tilde{s} \quad \vee \quad 5 < \tilde{r}
 \end{aligned}$$

Two galaxy clusters from Paper I, ABELL 2199 and WBL 514, present two evident galaxy systems in their surroundings between $\sim 2r_{200}$ and $\sim 3r_{200}$ (see Figures 1 and 2 in Paper I). In the case of WBL 514, this galaxy system corresponds to the cluster WBL 518 located $\sim 2^\circ$ west on the sky with coordinates $(\alpha, \delta)_{J2000} = (14\text{h } 40\text{m } 43.1\text{s}, +03\text{d } 27\text{m } 11\text{s})$ and a central redshift of $z=0.027$. The cluster ABELL 2199 has the cluster ABELL 2197 in their surroundings, located $\sim 1.5^\circ$ of projected distance, their coordinates are $(\alpha, \delta)_{J2000} = (16\text{h } 28\text{m } 10.4\text{s}, +40\text{d } 54\text{m } 26\text{s})$ and has a redshift of $z=0.0308$. These two galaxy systems, WBL 518 and ABELL 2197, are not included in the set of clusters from Paper I according to the constrain of being observed by the SDSS-DR6 and by the GALEX-AIS throughout sky regions corresponding to several megaparsecs. The central regions of these galaxy systems can be only inhabited by the typical galaxy population of the central regions of galaxy clusters. In order to avoid the mix between galaxy population from virial regions and from infall regions, we exclude the galaxy subsample of these two clusters from the galaxy sample corresponding to the infall regions. Specifically, we exclude from the infall regions those galaxies with the following coordinates:

$$\begin{aligned}
 \text{ABELL 2197:} & \quad 40.4 < \alpha_{J2000}(\text{°}) < 41.8 \quad \wedge \quad 245.8 < \delta_{J2000}(\text{°}) < 248.0 \\
 \text{WBL 518:} & \quad 3.0 < \alpha_{J2000}(\text{°}) < 4.2 \quad \wedge \quad 219.8 < \delta_{J2000}(\text{°}) < 220.75
 \end{aligned}$$

In Appendix, we show the results of the same analysis performed here but including the central regions of these clusters as part of the galaxy sample in the infall regions.

Figure 2 shows the distribution and the average trend of the $NUV - r'$ color for our sample of star-forming galaxies along their r' -band absolute magnitude $M_{r'}$ in the three

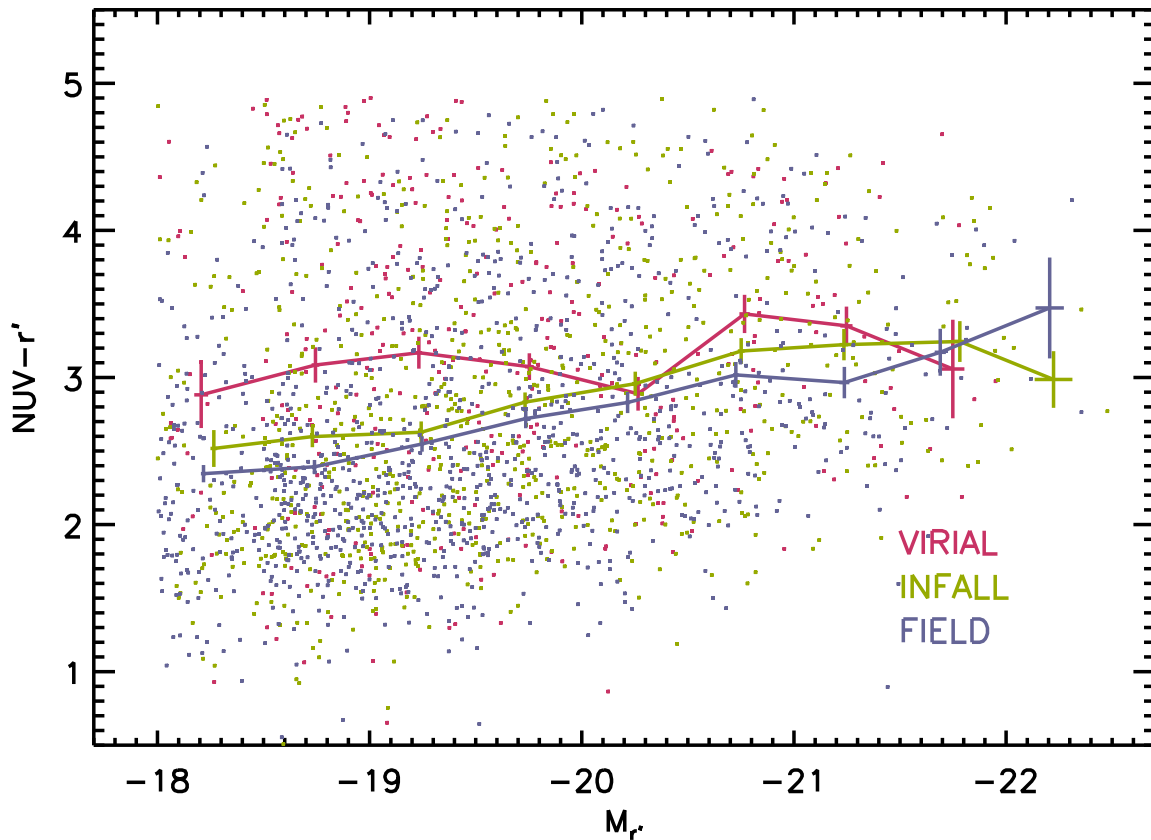


Fig. 2.— $NUV - r'$ vs. $M_{r'}$ of star-forming galaxies in each of the defined environments: virial regions (red), infall regions (green) and field environment (blue). Each point corresponds to one galaxy from the environment identified by its color. The data points correspond to the mean of $NUV - r'$ in each luminosity bin. The vertical and horizontal bars correspond to the bootstrap uncertainties in the mean of $NUV - r'$ and in the mean of $M_{r'}$, respectively, in each luminosity bin (see text for details).

different environments. In order to be complete in each luminosity bin, we select only those star-forming galaxies fulfilling the two following conditions: (i) galaxies whose r' -band composite-model absolute magnitude, $M_{r'}$, is inside the limits (lower limit - $M_{r'}^{lbin}$; upper limit - $M_{r'}^{ubin}$) of each luminosity bin,

$$M_{r'}^{lbin} < M_{r'} \leq M_{r'}^{ubin} \quad (2)$$

and (ii) galaxies from those clusters for which their completeness limit of the r' -band composite-model absolute magnitude $M_{r'}^{clim}$ is fainter than the upper limit of each luminosity bin $M_{r'}^{ubin}$,

$$M_{r'}^{ubin} \leq M_{r'}^{clim} \quad (3)$$

In order to compute $M_{r'}^{clim}$, we assume the completeness limit of the Main Galaxy Sample $r'=17.77$ and a conservative cut of $r' - r'_{cm}=0.21$ in the difference between the r' -band composite-model magnitude, r'_{cm} , and the r' -band petrosian magnitude r' . This cut embraces $\approx 90\%$ of the overall sample of cluster galaxies and $\approx 92.5\%$ of galaxies from the faintest bin, $17 < r' < 17.77$, or the optical-selected blue galaxies $u' - r' < 2.22$, as can be seen in Figure 3.

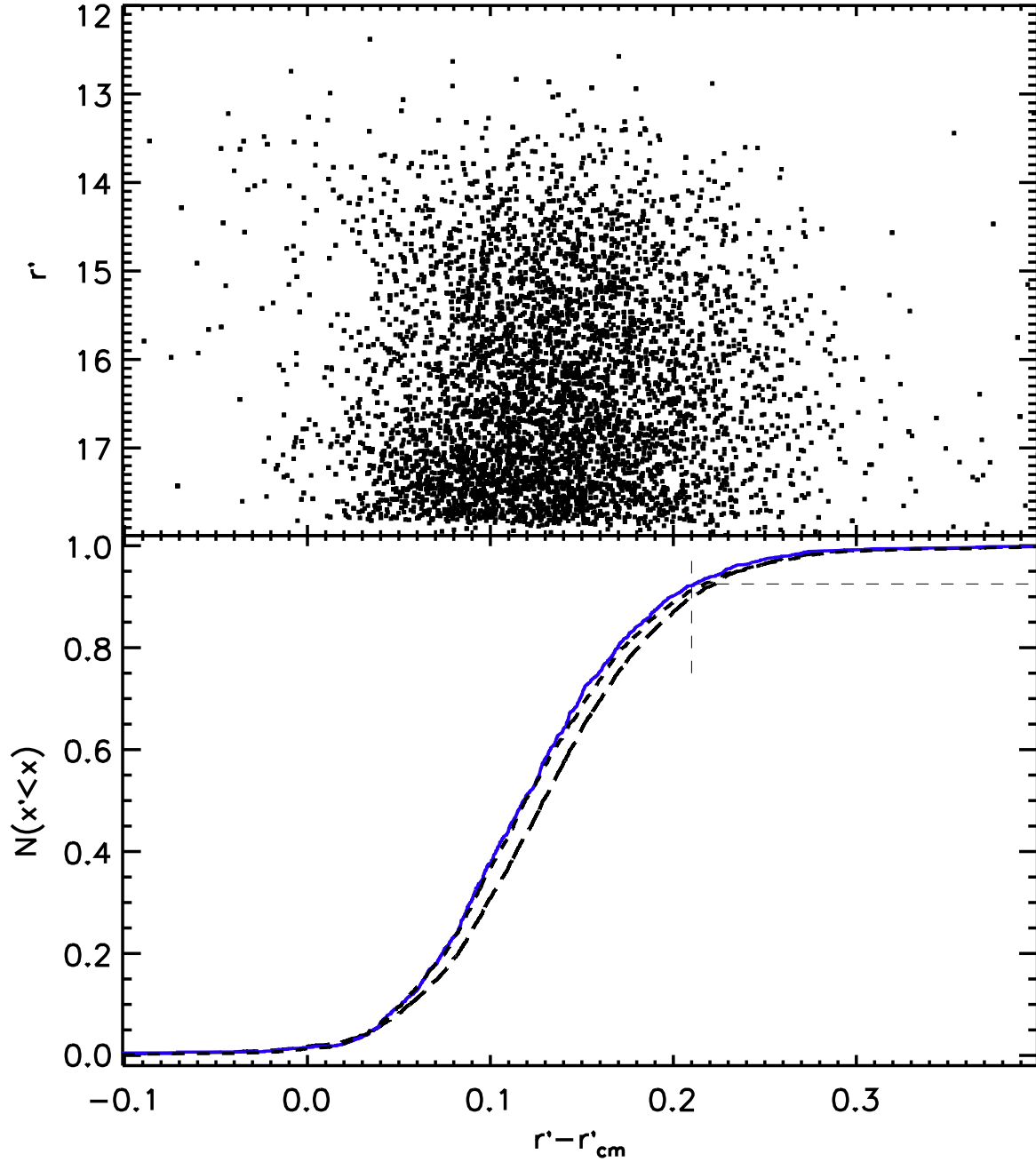


Fig. 3.— The description of this figure is in the following page.

Fig. 3.— **Top panel:** r' vs. $r' - r'_{cm}$ distribution of the sample of cluster galaxies. **Bottom panel:** Cumulative distribution fraction $N(x' < x)$ of $r' - r'_{cm}$ for the sample of cluster galaxies. The three curves corresponds to three different samples: the long-dashed curve shows the overall sample, the continuous blue curve shows the blue galaxies $u' - r' < 2.22$ and the short-dashed curve shows the faintest galaxies $17 < r' < 17.77$. The vertical and horizontal dashed lines correspond, respectively, to a magnitude difference of $r' - r'_{cm} = 0.21$ and a completeness of 92.5%.

Those galaxies for which a NUV detection is not available are discarded from our analysis. Those galaxies are not observed because they occupy the gaps between the circular GALEX fields or they are fainter than the completeness limit of GALEX-AIS. The first case does not introduce any bias since a correlation between the star formation properties of those galaxies and their celestial coordinates is not expected. In the second case, those galaxies are outside the color-magnitude locus dedicated to this study as you can see in Figure 4, assuming the AB-magnitude limit of a SDSS-GALEX matched catalogue $NUV \sim 22.5$ (Bianchi et al. 2007) and the completeness limit of the SDSS MGS in the r' -band composite-model magnitude $r'_{cm} = 17.56$

Figure 2 shows two clearly different behaviors in the $(NUV - r')$ - $(M_{r'})$ plane for star-forming galaxies depending on the environment where they inhabit. The average of $NUV - r'$ for the field star-forming galaxy sample follows a monotonic trend from $NUV - r' \sim 3.5$ at $M_{r'} \sim -22.25$ to $NUV - r' \sim 2.35$ at $M_{r'} \sim -18$. In the case of star-forming galaxies inhabiting the infall regions of clusters, they show a very similar trend to field star-forming galaxies, with a systematic bias of ~ 0.1 mag towards redder values of the $NUV - r'$ average. The trend of $NUV - r'$ average for star-forming galaxies from the virial regions show a distinct behavior: their $NUV - r'$ averages in the $M_{r'} < -20$ range are consistent with the $NUV - r'$ trend for infalling and field star-forming galaxies, within the uncertainties of $NUV - r'$ averages. In contrast, star-forming galaxies from virial regions in the $-20 < M_{r'} < -18$ range are systematically biased toward redder values of $NUV - r'$ in ~ 0.5 mag.

In order to accomplish an analysis in depth of the $NUV - r'$ distribution along the $M_{r'}$ range throughout the defined cluster regions, we split the star-forming galaxy sample in three luminosity intervals: the high-luminosity (HL) bin with $M_{r'} \leq -20$, the intermediate-luminosity (IL) bin with $-20 < M_{r'} \leq -19$, and the low-luminosity (LL) bin with

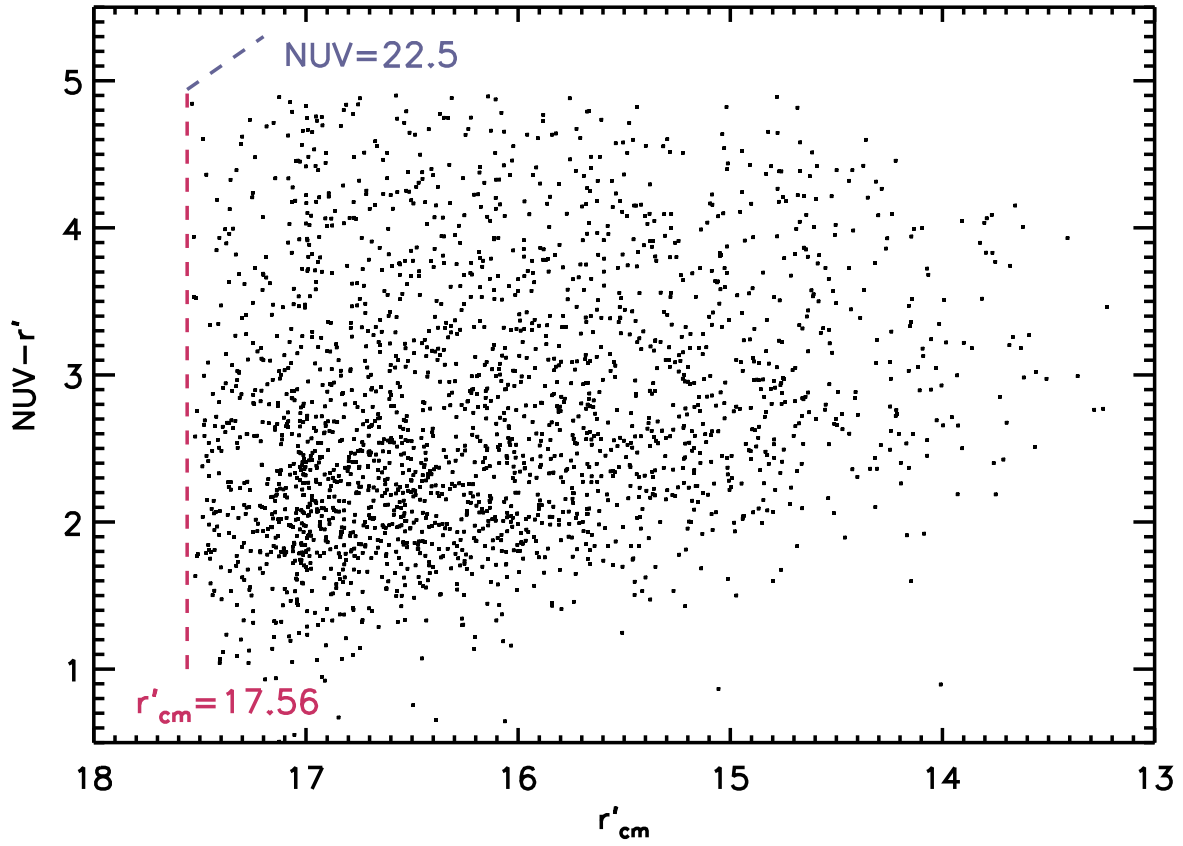


Fig. 4.— $NUV - r'$ vs. r'_{cm} of the star-forming galaxy sample. The red vertical dashed line corresponds to the SDSS MGS limit in r'_{cm} magnitude and the blue diagonal dashed line corresponds to the GALEX-AIS limit in NUV magnitude.

$-19 < M_{r'} \leq -18.2$. We choose the lowest luminosity cut, $M_{r'} = -18.2$, in order to maximize the size of the sample of star-forming galaxies in this bin, according to Eq. 2 and 3. Figure 5 shows the $NUV - r'$ distributions of star-forming galaxies for these three luminosity bins in the three environmental regions defined above; in Table 2 we show the averages and their bootstrap uncertainties for the distributions of each subsample.

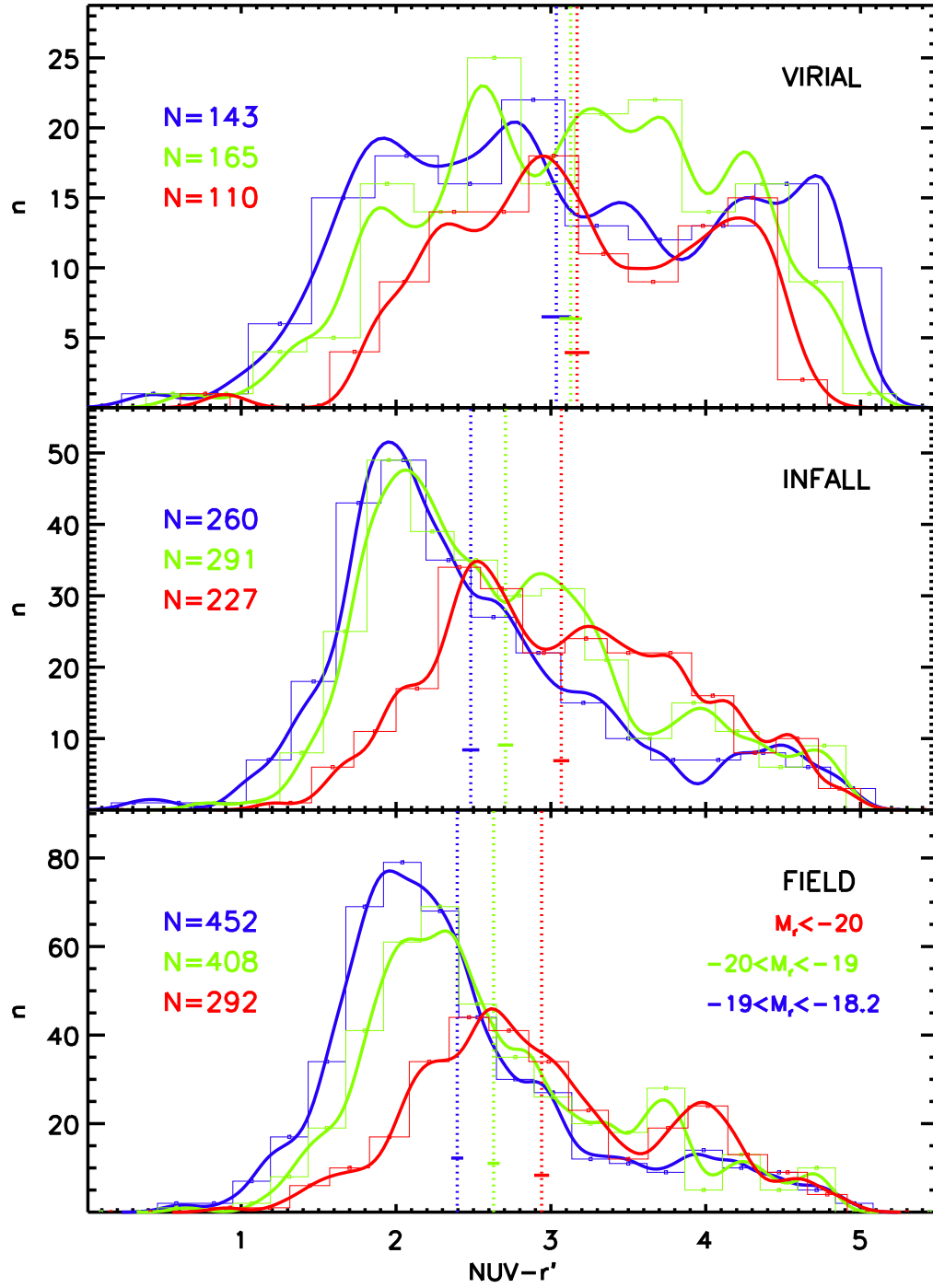


Fig. 5.— The description of this figure is in the following page.

Fig. 5.— $NUV - r'$ distributions of star-forming galaxies in each luminosity bin in the environmental regions defined above. The three different panels correspond to the three different environments, from the top to bottom: the virial regions, the cluster infall regions and the field environment. Color code identifies the three luminosity bins; red $M_{r'} \leq -20$, green $-20 < M_{r'} \leq -19$ and blue $-19 < M_{r'} \leq -18.2$. The thin lines correspond to the histograms in each case; the width of the bins are computed according to the rule $\Delta_H = \sigma/n^{1/5}$ (Turlach 1993) with σ and n the standard deviation and number of elements of distribution, respectively. The solid curves are the kernel density estimators computed with a gaussian kernel of $\sigma_{gauss} = \Delta_H$. The vertical dashed lines and the horizontal error bar represent, in each case, the average and its bootstrap uncertainty for each galaxy subsample, respectively. Numbers in the left upper corner of each panel show the total number of galaxies in each subsample.

As it is shown in Figure 5 and it can be seen in Table 2, two monotonic trends arise from these results: (i) At all luminosities, the average $NUV - r'$ reddens from the field environment to the virial regions (ii) For a given environment, the average $NUV - r'$ reddens as we move from LL to HL star-forming galaxies. The first trend, follows the general trend shown in the color-magnitude diagrams by the "blue cloud" (e.g. Baldry et al. 2004; Haines et al. 2008). Despite the small differences, the average $NUV - r'$ measured for HL galaxies in the three environments are consistent within one σ . This does not seem to be the case for IL and LL galaxies, where the average $NUV - r'$ of infall and field galaxies is clearly bluer than that of virial galaxies, and this behavior is more pronounced for LL than for IL galaxies. In addition, the $NUV - r'$ distributions for IL and LL galaxies present a maximum around $NUV - r'=2$ in infall and field environments. This maximum is clearly absent in the virial environment, where the $NUV - r'$ distributions present a top-hat shape at all luminosity ranges.

4. Discussion

In the previous section we have shown that the $NUV - r'$ distributions of galaxies in different environments present significant differences depending on the r' -band luminosity considered. In order to accomplish a rigorous analysis based on the $NUV - r'$ distributions, we apply a Kolmogorov-Smirnov (K-S) test. Table 3 shows the results from the K-S test when comparing the samples corresponding to the three environments for each luminosity bin. Figure 6 illustrates the results of the K-S test by showing a simplified scheme of the probability that the star-forming galaxy subsamples of same luminosity bin in different environments come from the same population. In what follows we discuss the implications of these results for the different luminosity bins.

Table 2: Averages and average uncertainties of $NUV - r'$ distributions for each luminosity bin in each environmental region.

Environment	$\langle NUV - r' \rangle$	\pm	$\sigma_{bootstrap}$
(1)	(2)		(3)
HL ($M_{r'} \leq -20$)			
Virial	3.169	\pm	0.080
Infall	3.067	\pm	0.052
Field	2.940	\pm	0.048
IL ($-20 < M_{r'} \leq -19$)			
Virial	3.128	\pm	0.073
Infall	2.707	\pm	0.050
Field	2.630	\pm	0.038
LL ($-19 < M_{r'} \leq -18.2$)			
Virial	3.035	\pm	0.095
Infall	2.483	\pm	0.055
Field	2.395	\pm	0.039

(1) Environmental region. (2) Mean of $NUV - r'$ distribution in the corresponding environmental region. (3) Bootstrap uncertainty of the corresponding $NUV - r'$ mean.

Table 3: Results from Kolmogorov-Smirnov test.

Subsamples	$D_{n1,n2}$	$P(x_{i1}, x_{i2})$
(1)	(2)	(3)
HL ($M_{r'} \leq -20$)		
Virial - Infall	0.100	0.429
Infall - Field	0.117	0.0570
Virial - Field	0.162	0.0256
IL ($-20 < M_{r'} \leq -19$)		
Virial - Infall	0.245	$4.75 \cdot 10^6$
Infall - Field	0.076	0.268
Virial - Field	0.295	$1.56 \cdot 10^9$
LL ($-19 < M_{r'} \leq -18.2$)		
Virial - Infall	0.285	$3.96 \cdot 10^7$
Infall - Field	0.081	0.214
Virial - Field	0.334	$3.38 \cdot 10^{11}$

(1) Environmental regions where the K-S is applied to the $NUV - r'$ distributions of their galaxies subsamples. (2) Maximum difference between the two cumulative distribution functions of the $NUV - r'$ distributions. (3) Probability that the two $NUV - r'$ distributions came from the same parent population.

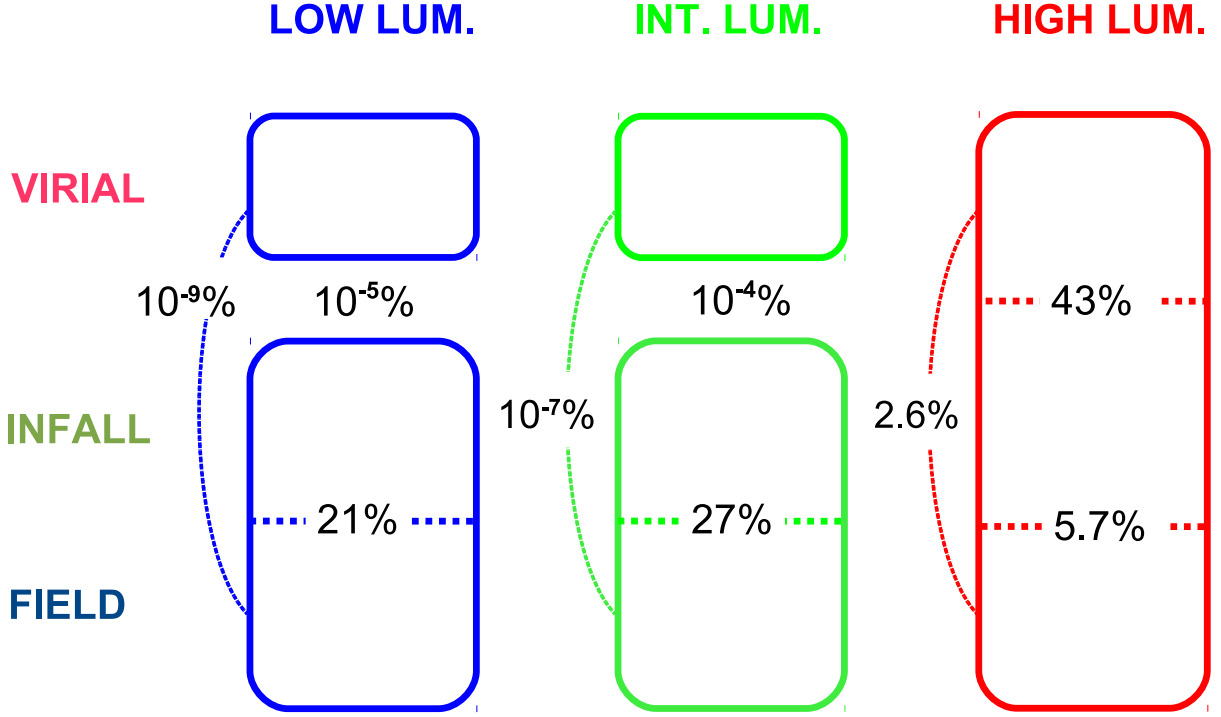


Fig. 6.— Simplified scheme of the statistical similarity between the $NUV - r'$ distributions of star-forming galaxy subsamples of the same luminosity bin from the different environmental regions. The figures on the picture are the K-S probabilities that the distributions came from the same parent population. The star-forming galaxy subsamples correspond, from left to right, to the low-luminosity bin $-19 < M_{r'} \leq -18.2$, the intermediate-luminosity bin $-20 < M_{r'} \leq -19$ and the high-luminosity bin $M_{r'} \leq -20$ and; from the top to the bottom, to the virial regions, the infall regions and the field environment. Monolithic blocks represent of star-forming galaxy subsamples presenting a significant similarity in their $NUV - r'$ distributions (see the text for details).

4.1. HL star-forming galaxies

In the case of HL ($M_{r'} \leq -20$) star-forming galaxies, the probability $P(x_{1i}, x_{2i})$ that the $NUV - r'$ distribution of the virial regions and the infall regions came from the same parent population is $P \approx 43\%$, so they show a high similarity in their $NUV - r'$ distributions. When comparing the infall regions and the field environment, this probability lowers to $P(x_{1i}, x_{2i}) \approx 6\%$, so we can not reject the null hypothesis that the distributions came from the same parent population. The comparison between the virial regions and the field environment yields a probability $P(x_{1i}, x_{2i}) \approx 3\%$, which is still low but it does not allow to reject the null hypothesis. All these results point out that the HL star-forming galaxies, from the point of view of the environmental influence on their $NUV - r'$ distributions, form a unique family of galaxies only subtly affected by the environment where they inhabit. They only show a very mild gradient of reddening towards the inner parts of galaxy clusters. Assuming that the $NUV - r'$ distributions of the HL star-forming galaxies as our unique observable, we propose two scenarios about the environmental influence on the star formation activity of these galaxies: (1) there is not a strong environmental influence on the star formation activity of these galaxies in the last $\sim 10^8$ yr or (2) the environmental processes which would affect these galaxies act on short time-scales, taking as a reference the time-scale of UV luminosity, $\tau_{UV} \sim 10^8$ yr.

A sudden truncation of a previously significant star formation in the last 1.5 Gyr leaves (at least) two observable imprints on the galaxy spectrum: strong Balmer lines in absorption ($EW_{H\delta} > 3 \text{ \AA}$) and negligible emission lines (e.g. [OII]) (Poggianti et al. 2004); this kind of galaxies have been named *k+a* galaxies (in the modern designation, Dressler et al. 1999) or E+A galaxies (as they were first identified by Dressler & Gunn 1983). Because of this, the *k+a* spectra are often linked with *poststarburst* galaxies. Those galaxies have an specific locus in an UV-optical color-color diagram (e.g. GALEX-SDSS

color diagram). Their optical colors are as blue as the blue-cloud galaxies and their UV-optical colors are as red as the red-sequence galaxies (Kaviraj et al. 2007a). As you can see in Figure 7, the appearance of our sample of HL galaxies in such color-color diagram shows that this kind of galaxies are clearly absent in the observed locus for $k+a$ galaxies found by Kaviraj et al. (2007a, see their figure 1). This is in agreement with other results found for local galaxy clusters (e.g. Fabricant et al. 1991). In contrast, the luminous $k+a$ galaxies are abundant in the field (e.g. Goto 2005) and also they represent a significant fraction of the cluster dwarf galaxy population in Coma cluster (Poggianti et al. 2004). Summarizing, a short time-scale mechanism quenching star formation (i.e. gas stripping) in HL star-forming galaxies is not expected to have affected significantly those galaxies in the last ~ 1.5 Gyr.

4.2. IL star-forming galaxies

In the case of IL ($-20 < M_{r'} \leq -19$) star-forming galaxies, there is a high similarity between the $NUV - r'$ distribution of this subsample of galaxies inhabiting the infall regions and the corresponding one inhabiting the field environment, $P(x_{1i}, x_{2i}) \approx 27\%$. Contrarily, the comparison of virial and infall galaxies yields a probability of $P(x_{1i}, x_{2i}) \sim 10^{-4}\%$, similar to the one arising from the comparison of virial and field galaxies ($P(x_{1i}, x_{2i}) \sim 10^{-7}\%$). These results imply that the infall and field distributions do not come from the same parent population as the virial one. These results suggest there is an environmental mechanism strongly affecting the star formation activity of the galaxies inside the virial regions on time-scales of 10^8 yr. Following the scheme proposed by Treu et al. (2003) for the radial range where each environmental process predominantly operates, we propose starvation through the interaction with the ICM and the DMH as the main environmental process which affects those galaxies in the virial regions. In addition, a systematic reddening is

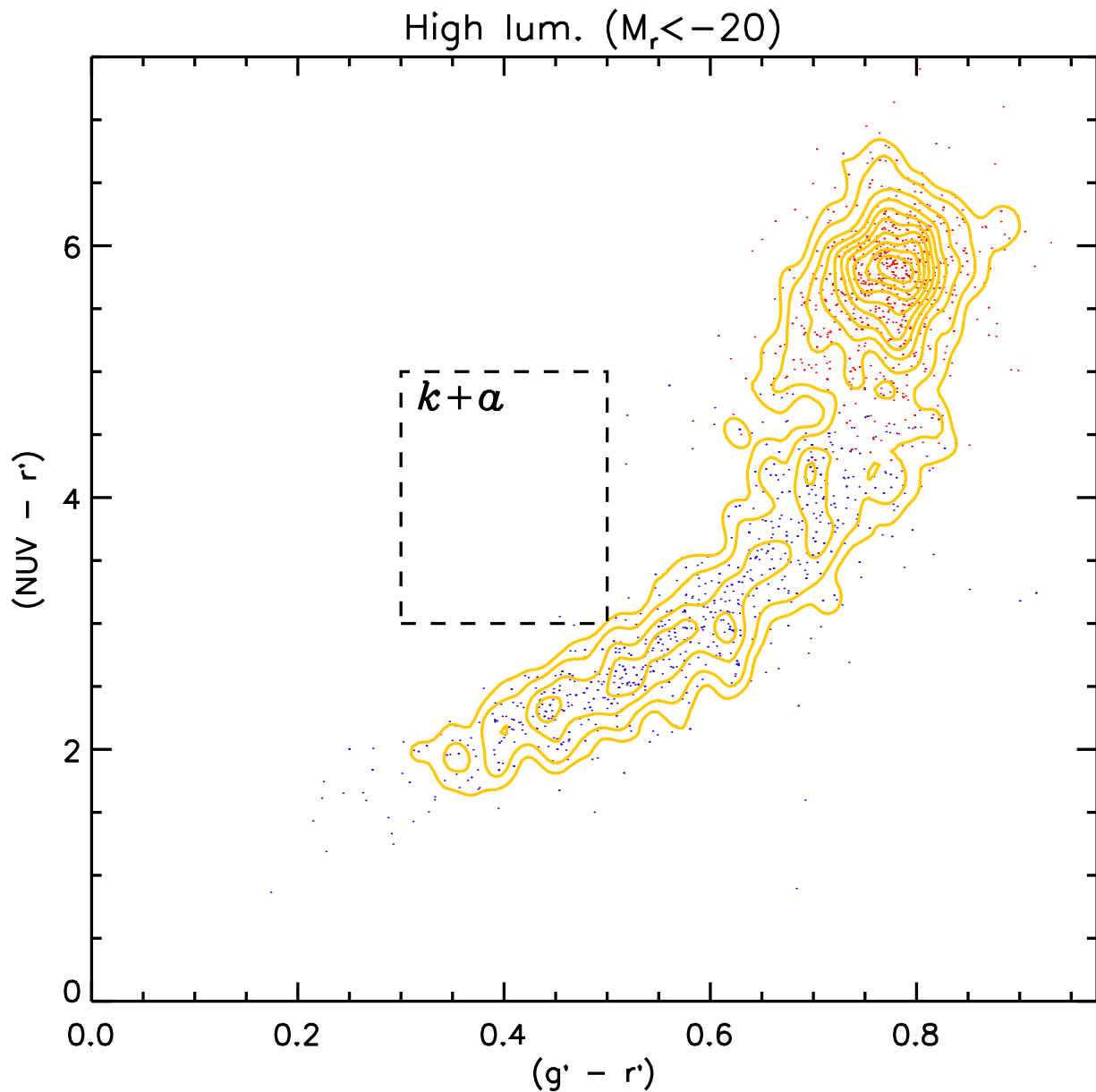


Fig. 7.— $(NUV - r')$ vs. $(g' - r')$ for the $M_{r'} < -20$ galaxy sample. Yellow isocontours represents the isodensity contours of HL galaxies. Blue and red points represent, respectively, star-forming and passive galaxies under the prescription shown in Section 3. The square box represents the locus of the $k+a$ galaxies in this color-color diagram (Kaviraj et al. 2007a, Fig. 1).

observed for star-forming galaxies in this luminosity bin, $-20 < M_{r'} \leq -19$, with respect to the field star-forming galaxies. This is not just observed in the virial region, but it is observed in the infall region as well. This result suggests there is some environmental process not just acting in the virial region but in the infall region too. Again, following the scheme proposed by Treu et al. (2003) for the radial range for each environmental process, we propose galaxy harassment as the environmental process quenching the star formation activity of IL star-forming-galaxies in the virial and the infall regions.

4.3. LL star-forming galaxies

The results from the K-S test applied to the LL ($-19 < M_{r'} \leq -18.2$) star-forming galaxies show a similar scheme to those shown by the IL star-forming galaxies. The LL star-forming galaxies from the virial regions present a $NUV - r'$ distribution clearly different from those ones from the infall regions and the field environment. The probability of coming from the same parent population between virial and infall regions is $P(x_{1i}, x_{2i}) \sim 10^{-5}$, while this probability goes down to $P(x_{1i}, x_{2i}) \sim 10^{-9}$ for the pair: virial regions vs. field environment. However, there is a significant similarity between the $NUV - r'$ distributions from the infall regions and from the field environment with a probability of $P(x_{1i}, x_{2i}) \approx 21\%$. Even though, these galaxies seem to suffer a stronger quenching in their star formation activity than the IL star-forming galaxies. The reddening of the $NUV - r'$ averages towards the inner parts of the clusters is larger for the LL star-forming galaxies than for the IL star-forming galaxies, assuming the galaxies from the virial regions as the reference, including the gross differences and those normalized to the sum of the uncertainties, see Table 2. The comparison of the virial regions with the field environment produces a difference normalized to the sum of uncertainties Δ/σ of 4.449 and 4.767 for the IL and the LL star-forming galaxies, respectively. The comparison of the virial regions with the infall regions produces

a Δ/σ of 3.42190 and 3.67115 for the IL and for the LL star-forming galaxies, respectively.

The proposed environmental mechanisms which can affect more strongly the LL star-forming galaxies seem to be (in the same way as the IL star-forming galaxies) the galaxy harassment - in order to explain the reddening in the infall regions with respect to the field environment - and the starvation, through the interaction with the ICM and through interaction with the DMH - to explain the evident difference in the $NUV - r'$ distributions between the virial regions and the other environmental regions.

As mentioned above, the effects of environment in the quenching of star formation activity seem to be more pronounced on the LL star-forming galaxies than on the IL star-forming galaxies. This suggests that the intensity of the above-cited environmental processes has some dependence on the galaxy luminosity or on the galaxy (stellar or gravitational) mass. In the case of galaxy harassment, Moore et al. (1999) found, through equilibrium high-resolution model of spirals embedded in a N-body simulation, that the response of a spiral galaxy to tidal encounters depends primarily on the central depth of its gravitational potential and its disc scale-length, mainly determined by the stellar component of galaxies. Low-surface brightness galaxies evolve dramatically under the influence of rapid encounters with substructures and strong tidal shocks from the global cluster potential (i.e. galaxy harassment), while high-surface brightness galaxies are more stable to the galaxy stirring in clusters and to the tidal encounters. In the case of starvation, Bekki et al. (2002) performed numerical simulations to evaluate the stripping which the hot halo gas undergoes when subjected to both the ram pressure of the ICM and the global tidal field of the cluster. According to this work, the less massive a galaxy is, the more efficient those mechanisms are (ICM stripping, Bekki et al. 2002 and tidal halo stripping, Byrd & Valtonen 1990; Henriksen & Byrd 1996; Byrd & Valtonen 2001). In conclusion, the proposed environmental processes acting on IL and LL star-forming galaxies match the fact

that they produce the stronger effects on star formation activity for the LL star-forming galaxies.

5. Summary and conclusions

In this paper, we expose an original approach which analyzes the $NUV - r'$ distributions of a large sample of star-forming galaxies in clusters covering a range of more than four r' -band magnitudes down to $M_{r'} \sim -18$ and distributed in three distinct environmental regions: the virial regions, the cluster infall regions and the field environment. According to the characteristics of each environmental process, we discuss and propose which environmental processes affect the star-forming galaxies depending on their luminosity. In the following summary, we present the main results and conclusions of this work.

- The similarity of the $NUV - r'$ distributions of HL ($M_{r'} \leq -20$) star-forming galaxies in the different environmental regions together with the absence of luminous $k+a$ galaxies in our cluster galaxy sample point out that there is neither a strong environmental influence on the star formation activity of these galaxies in the last $\sim 10^8$ yr nor a sudden truncation of star formation in the last 1.5 Gyr.
- The $NUV - r'$ distributions of IL ($-20 < M_{r'} \leq -19$) star-forming galaxies from the infall regions and the field environment show a remarkable similarity. In contrast, the $NUV - r'$ distributions of IL star-forming galaxies in virial regions are clearly distinct from the corresponding ones in infall regions and in the field environment. This behavior of the $NUV - r'$ distributions of IL star-forming galaxies points out the starvation through the combined interaction with the ICM and the DMH as the environmental process quenching significantly the star formation activity of IL star-forming galaxies in the virial regions of clusters. The reddening of $NUV - r'$

distributions of these galaxies observed not just in the virial regions, but even in the infall regions with respect to the field environment is an indication of there is some environmental process acting on these galaxies (at least) in the infall region. The galaxy harassment as long-time-scale process $\tau \gtrsim 10^8$ yr is a suitable candidate to be responsible of the observed differences in the $NUV - r'$ distributions.

- The LL ($-19 < M_{r'} \leq -18.2$) star-forming galaxies present the same trends of IL star-forming galaxies in their $NUV - r'$ distributions. Consequently, we propose that the same environmental processes in the same environmental regions are affecting the star-formation activity of these galaxies. Even more, the $NUV - r'$ averages of the LL star-forming galaxies in the virial regions show a stronger reddening with respect to the infall regions and the field environment than the IL star-forming galaxies. Indeed, the observed effect of these environmental processes (starvation, harassment) are stronger for low luminosity galaxies.

To conclude, we claim that our results highlight the added value of a sample of cluster galaxies mapping a broad variety of environmental conditions with a large range in galaxy luminosity and with multi-wavelength (from UV to FIR) available data.

Acknowledgments

J.D.H.F. thanks L'Osservatorio Astronomico di Padova for hospitality during the stays where this work was started. We want especially thank Bianca M^a Poggianti for their help and advice during this stay. J.D.H.F. acknowledges financial support from the Spanish Ministerio de Ciencia e Innovación under the FPI grant BES-2005-7570. We also acknowledge funding by the Spanish PNAYA project ESTALLIDOS (grants AYA2007-67965-C03-02, AYA2010-21887-C04-01) and project CSD2006 00070 “1st Science

with GTC” from the CONSOLIDER 2010 program of the Spanish MICINN.

This publication has made use of the following resources:

- the NASA/IPAC Extragalactic Database (NED) which is operated by the Jet Propulsion Laboratory, California Institute of Technology, under contract with the National Aeronautics and Space Administration.
- the Sloan Digital Sky Survey (SDSS) database. Funding for the Sloan Digital Sky Survey (SDSS) and SDSS-II has been provided by the Alfred P. Sloan Foundation, the Participating Institutions, the National Science Foundation, the U.S. Department of Energy, the National Aeronautics and Space Administration, the Japanese Monbukagakusho, and the Max Planck Society, and the Higher Education Funding Council for England. The SDSS Web site is <http://www.sdss.org/>.

The SDSS is managed by the Astrophysical Research Consortium (ARC) for the Participating Institutions. The Participating Institutions are the American Museum of Natural History, Astrophysical Institute Potsdam, University of Basel, University of Cambridge, Case Western Reserve University, The University of Chicago, Drexel University, Fermilab, the Institute for Advanced Study, the Japan Participation Group, The Johns Hopkins University, the Joint Institute for Nuclear Astrophysics, the Kavli Institute for Particle Astrophysics and Cosmology, the Korean Scientist Group, the Chinese Academy of Sciences (LAMOST), Los Alamos National Laboratory, the Max-Planck-Institute for Astronomy (MPIA), the Max-Planck-Institute for Astrophysics (MPA), New Mexico State University, Ohio State University, University of Pittsburgh, University of Portsmouth, Princeton University, the United States Naval Observatory, and the University of Washington.

- the Galaxy Evolution Explorer (GALEX), which is a NASA mission managed by the Jet Propulsion Laboratory and launched in 2003 April. We gratefully acknowledge

NASA’s support for the construction, operation, and science analysis for the GALEX mission, developed in cooperation with the Centre National d’Etudes Spatiales of France and the Korean Ministry of Science and Technology.

Appendix

In this appendix, we show the results about the same analysis developed in this work including the central regions of the clusters ABELL 2197 and WBL 518 as part of the galaxy sample in the infall regions.

Table 4 shows the averages (and uncertainties) of $NUV - r'$ distributions for each luminosity bin of star-forming galaxies in each environmental region and the table 5 show the results of the K-S test applied to these galaxy subsamples.

As you can see, the data corresponding to infall regions (the only line modified in this section) shows, systematically, redder $NUV - r'$ averages than the averages in the previous analysis in the three luminosity bins. This is in agreement with the motivation of the extraction of the central regions of these clusters from the cluster infall regions of their companions; in these excluded regions inhabit the typical ”red” galaxy population from the central cluster regions. Anyway, the differences are lower than the associated uncertainties, except for the case of the LL star-forming galaxies whose difference is $\approx 2\sigma$.

In the case of results from the K-S test, the changes in the probabilities in each case point out the extraction of clusters ABELL 2197 and WBL 518 from the infall regions of their neighbor clusters as a good approach. The probabilities of the $NUV - r'$ distributions of star-forming galaxy subsamples from the virial region and from the infall regions of came from the same parent population increase with respect to the previous analysis, while the probabilities of the $NUV - r'$ distributions of star-forming galaxy subsamples from the

Table 4: Averages and uncertainties of distributions of $NUV - r'$ environments.

Environments	$\langle NUV - r' \rangle$	\pm	$\sigma_{bootstrap}$
HL ($M_r \leq -20$)			
Virial	3.169	\pm	0.080
Infall	3.097	\pm	0.049
Field	2.940	\pm	0.048
IL ($-20 < M_r \leq -19$)			
Virial	3.128	\pm	0.073
Infall	2.723	\pm	0.051
Field	2.630	\pm	0.038
LL ($-19 < M_r \leq -18.2$)			
Virial	3.035	\pm	0.095
Infall	2.601	\pm	0.052
Field	2.395	\pm	0.039

Table 5: Results from Kolmogorov-Smirnov test, including the central regions of ABELL 2197 and WBL 518 as part of the galaxy sample in the infall regions.

Subsamples	D_{n_1, n_2}	$P(x_{i_1}, x_{i_2})$
(1)	(2)	(3)
HL ($M_{r'} \leq -20$)		
Virial - Infall	0.086	0.601
Infall - Field	0.137	0.0106
Virial - Field	0.162	0.0260
IL ($-20 < M_{r'} \leq -19$)		
Virial - Infall	0.241	$5.13 \cdot 10^6$
Infall - Field	0.083	0.172
Virial - Field	0.295	$1.56 \cdot 10^9$
LL ($-19 < M_{r'} \leq -18.2$)		
Virial - Infall	0.232	$4.28 \cdot 10^5$
Infall - Field	0.130	0.00377
Virial - Field	0.334	$3.38 \cdot 10^{11}$

(1) Environmental regions where the K-S is applied to the $NUV - r'$ distributions of their galaxies subsamples. (2) Maximum difference between the two cumulative distribution functions of the $NUV - r'$ distributions. (3) Probability that the two $NUV - r'$ distributions came from the same parent population.

infall regions and the field environment decrease systematically in the all luminosity bins. These issues suggest the inclusion of ABELL 2197 and WBL 518 in the infall regions makes the $NUV - r'$ distributions more similar between the infall regions and the virial regions, in the same way it makes the $NUV - r'$ distributions of the infall regions more different from those from the field environment. Therefore, the central regions of these clusters have a higher similarity in the $NUV - r'$ distributions of their star-forming galaxy population with the virial regions than the infall regions, as we suppose in our approach.

REFERENCES

- Abadi, M. G., Moore, B., & Bower, R. G. 1999, MNRAS, 308, 947
- Abazajian, K., Adelman-McCarthy, J. K., Agüeros, M. A., et al. 2004, AJ, 128, 502
- Adelman-McCarthy, J. K., Agüeros, M. A., Allam, S. S., et al. 2008, ApJS, 175, 297
- Baldry, I. K., Glazebrook, K., Brinkmann, J., et al. 2004, ApJ, 600, 681
- Bekki, K. 1998, ApJ, 502, L133
- Bekki, K., Couch, W. J., & Shioya, Y. 2002, ApJ, 577, 651
- Bertin, E. & Arnouts, S. 1996, A&AS, 117, 393
- Bianchi, L., Rodriguez-Merino, L., Viton, M., et al. 2007, ApJS, 173, 659
- Boselli, A. & Gavazzi, G. 2006, PASP, 118, 517
- Buat, V., Iglesias-Páramo, J., Seibert, M., et al. 2005, ApJ, 619, L51
- Byrd, G. & Valtonen, M. 1990, ApJ, 350, 89
- Byrd, G. & Valtonen, M. 2001, AJ, 121, 2943
- Chilingarian, I. V. & Zolotukhin, I. Y. 2012, MNRAS, 419, 1727
- Cortese, L., Gavazzi, G., Boselli, A., Iglesias-Paramo, J., & Carrasco, L. 2004, A&A, 425,
429
- den Hartog, R. & Katgert, P. 1996, MNRAS, 279, 349
- Diaferio, A. 1999, MNRAS, 309, 610
- Dressler, A. 1980, ApJ, 236, 351

- Dressler, A. & Gunn, J. E. 1983, *ApJ*, 270, 7
- Dressler, A., Smail, I., Poggianti, B. M., et al. 1999, *ApJS*, 122, 51
- Evrard, A. E. 1991, *MNRAS*, 248, 8P
- Fabricant, D. G., McClintock, J. E., & Bautz, M. W. 1991, *ApJ*, 381, 33
- Fujita, Y. 1998, *ApJ*, 509, 587
- Ghigna, S., Moore, B., Governato, F., et al. 1998, *MNRAS*, 300, 146
- Gómez, P. L., Nichol, R. C., Miller, C. J., et al. 2003, *ApJ*, 584, 210
- Goto, T. 2005, *MNRAS*, 357, 937
- Haines, C. P., Gargiulo, A., & Merluzzi, P. 2008, *MNRAS*, 385, 1201
- Henriksen, M. & Byrd, G. 1996, *ApJ*, 459, 82
- Hernández-Fernández et al. 2012, UV to FIR catalogue of a galaxy sample in nearby clusters: SEDs and environmental trends (accepted, arXiv:1201.2697)
- Icke, V. 1985, *A&A*, 144, 115
- Iglesias-Páramo, J., Buat, V., Takeuchi, T. T., et al. 2006, *ApJS*, 164, 38
- Kaiser, N. 1987, *MNRAS*, 227, 1
- Kauffmann, G., Heckman, T. M., Budavári, T., et al. 2007, *ApJS*, 173, 357
- Kaviraj, S., Kirkby, L. A., Silk, J., & Sarzi, M. 2007a, *MNRAS*, 382, 960
- Kaviraj, S., Rey, S., Rich, R. M., Yoon, S., & Yi, S. K. 2007b, *MNRAS*, 381, L74
- Kennicutt, Jr., R. C. 1998, *ARA&A*, 36, 189

- Larson, R. B., Tinsley, B. M., & Caldwell, C. N. 1980, *ApJ*, 237, 692
- Leitherer, C., Schaerer, D., Goldader, J. D., et al. 1999, *ApJS*, 123, 3
- Lewis, I., Balogh, M., De Propris, R., et al. 2002, *MNRAS*, 334, 673
- Mahdavi, A., Böhringer, H., Geller, M. J., & Ramella, M. 2000, *ApJ*, 534, 114
- Mahdavi, A. & Geller, M. J. 2001, *ApJ*, 554, L129
- Martin, D. C., Fanson, J., Schiminovich, D., et al. 2005, *ApJ*, 619, L1
- Merritt, D. 1984, *ApJ*, 276, 26
- Mihos, J. C. 1995, *ApJ*, 438, L75
- Mihos, J. C. 2004, *Clusters of Galaxies: Probes of Cosmological Structure and Galaxy Evolution*, 277
- Mihos, J. C. & Hernquist, L. 1994, *ApJ*, 431, L9
- Mihos, J. C. & Hernquist, L. 1996, *ApJ*, 464, 641
- Mo, H., van den Bosch, F. C., & White, S. 2010, *Galaxy Formation and Evolution* (Cambridge University Press. New York)
- Moore, B., Katz, N., Lake, G., Dressler, A., & Oemler, A. 1996, *Nature*, 379, 613
- Moore, B., Lake, G., & Katz, N. 1998, *ApJ*, 495, 139
- Moore, B., Lake, G., Quinn, T., & Stadel, J. 1999, *MNRAS*, 304, 465
- Natarajan, P., Kneib, J., Smail, I., & Ellis, R. S. 1998, *ApJ*, 499, 600

- Poggianti, B. M. 2006, in *The Many Scales in the Universe: JENAM 2004 Astrophysics Reviews*, ed. J. C. Del Toro Iniesta, E. J. Alfaro, J. G. Gorgas, E. Salvador-Sole, & H. Butcher, 71
- Poggianti, B. M., Bridges, T. J., Komiyama, Y., et al. 2004, *ApJ*, 601, 197
- Quilis, V., Moore, B., & Bower, R. 2000, *Science*, 288, 1617
- Rines, K., Geller, M. J., Kurtz, M. J., & Diaferio, A. 2003, *AJ*, 126, 2152
- Rines, K., Geller, M. J., Kurtz, M. J., & Diaferio, A. 2005, *AJ*, 130, 1482
- Salim, S., Charlot, S., Rich, R. M., et al. 2005, *ApJ*, 619, L39
- Stoughton, C., Lupton, R. H., Bernardi, M., et al. 2002, *AJ*, 123, 485
- Strateva, I., Ivezić, Ž., Knapp, G. R., et al. 2001, *AJ*, 122, 1861
- Strauss, M. A., Weinberg, D. H., Lupton, R. H., et al. 2002, *AJ*, 124, 1810
- Treu, T., Ellis, R. S., Kneib, J., et al. 2003, *ApJ*, 591, 53
- Turlach, B. A. 1993, in *CORE and Institut de Statistique*
- Wang, B. & Heckman, T. M. 1996, *ApJ*, 457, 645